

Analyzing the transport coefficients and observables of a rotating QGP medium in kinetic theory framework with a novel approach to the collision integral

Shubhalaxmi Rath^{*1} and Sadhana Dash^{†2}

¹Instituto de Alta Investigación, Universidad de Tarapacá, Casilla 7D, Arica, Chile

²Department of Physics, Indian Institute of Technology Bombay, Mumbai 400076, India

Abstract

In the present work, we have studied how the rotation of the QGP medium affects the transport coefficients and observables in heavy ion collisions. For the noncentral collisions, although most of the angular momentum gets carried away by the spectators, there still remains a finite angular momentum with a finite range of angular velocity, which thus incites rotation in the produced matter. As a result, various properties of the QGP medium are likely to be modulated by the rotation. We have calculated the transport coefficients and observables, such as the electrical conductivity, the thermal conductivity, the Knudsen number, the elliptic flow, the specific heat at constant pressure, the specific heat at constant volume, the trace anomaly, the thermal diffusion constant and the isothermal compressibility using the kinetic theory to see the effect of rotation on them. In particular, we have used the novel relaxation time approximation for the collision integral in the relativistic Boltzmann transport equation to derive the transport coefficients and compared them with their values in the relaxation time approximation within the kinetic theory approach in conjunction with the finite angular velocity. We have found that the angular velocity plays an important role and enhances the flow of charge and heat in the medium. Further, as compared to the relaxation time approximation, the electrical and thermal conductivities have smaller values in the novel relaxation time approximation and these differences between the conductivities in the said approximations are more pronounced at high temperature than at low temperature. Furthermore, all the aforesaid observables are found to be sensitive to the rotation of the QGP medium.

^{*}shubhalaxmirath@gmail.com

[†]sadhana@phy.iitb.ac.in

1 Introduction

The possibility of creating the extreme state of matter that existed in the beginning of the universe, *i.e.* quark-gluon plasma (QGP) in ultrarelativistic heavy ion collisions at Relativistic Heavy Ion Collider (RHIC) and Large Hadron Collider (LHC) has elevated the exploration and understanding of the properties of such matter. In addition, the study of the evolution of the primordial matter, its equation of state and the phase structure within the quantum chromodynamics (QCD) at finite temperature, density and other extreme conditions are some of the important goals of the heavy ion collisions. There exist evidences that, in the noncentral heavy ion collisions, the nuclei colliding at ultrarelativistic energies could possess a large initial angular momentum of the order $J \propto b\sqrt{s_{NN}}$, where b and $\sqrt{s_{NN}}$ are the impact parameter and the center-of-mass energy, respectively. Although a large part of the angular momentum is carried away by the spectators, there still a significant fraction of the angular momentum varying between $10^3\hbar$ and $10^5\hbar$ with angular velocity in the range 0.01 GeV - 0.1 GeV or even more is retained in the interaction zone due to the inhomogeneity of the colliding nuclei in the transverse plane, which further gets transferred to the produced fireball [1–4]. Thus, the larger overlap region between the colliding nuclei or impact parameter and large collision energy may result into higher angular momentum of the QGP. The fireball or the QGP may sustain the large angular momentum for a longer time due to the conservation of the total angular momentum. Thus, QGP may be perceived as a rotating system and accordingly, its properties could be significantly altered. Consequently, the initial angular momentum of the QGP may give rise to significant observable effects in heavy ion collisions, for example, global polarization of the thermal photons, dileptons and final hadrons with spin, enhancement of the elliptic flow and broadening of the transverse momentum spectra [5, 6]. Like the rotating QGP, other systems where rotating matter exists are the spinning neutron stars [7] and the nonrelativistic bosonic cold atoms [8]. Rotating QGP medium with finite magnetic field also induces some interesting phenomenological effects, such as chiral vortical effect [9, 10], chiral vortical wave [11], chiral magnetic effect [12, 13], chiral magnetic wave [14, 15], spin alignment of vector mesons [5], emission of circularly polarized photons [16] and spin polarization of observed particles in heavy ion collisions [17–22].

In a system, angular momentum exhibits the vorticity, and the coupling between the rotational motion and the quantum spin can result into polarization of hadrons, or in other words, the polarization of emitted hadrons in heavy ion collisions can be treated as a signature of vorticity in the produced matter. The initial conditions of the collisions, *i.e.* the energy and the impact parameter mainly decide the amount of polarization of observable particles. A review on the progress of theoretical and experimental activities

on the vortical behavior of the QGP is found in ref. [23]. The relativistic rotational effect could also influence the thermodynamics and the critical temperature of QGP to hadronic phase transition in QCD. The formulation of the finite temperature field theory in a rotating system can be found in ref. [24]. Most of the observations in different approaches, such as the Nambu-Jona-Lasinio model [3, 25], the local density approximation with the boundary condition [26], the hadron resonance gas model [27] and the holographic QCD approach [28] had found that the rotation decreases the critical temperature, whereas an increase of the critical temperature was reported in lattice simulations [29, 30]. According to the study using the Nambu-Jona-Lasinio model, it was estimated that the rotation also decreases the critical temperature of chiral symmetry breaking due to the suppression of chiral condensate in the similar regime [31]. Thus, like the high temperature, the strong magnetic field and large chemical potential, the rapid rotation of QGP matter can be treated as a kind of extreme condition. Out of different external conditions, magnetic field directly affects the quark degrees of freedom and indirectly affects the gluon degrees of freedom only through the quark loops, unlike the temperature that affects all degrees of freedom in QCD. The rotation could also affect quark as well as gluon degrees of freedom.

Recently, a lot of effort has been put into the investigation of various features of magnetized and fast rotating QCD matter due to the emergence of extremely strong magnetic field and large angular momentum in the noncentral events of heavy ion collisions. Both magnetic field and rotation would significantly alter the properties of hot and dense matter. Studies on the rotating free fermion states were carried out in references [18, 32–35], whereas the system of interacting fermions was studied in references [26, 31, 36] using effective field theoretical models, in references [37, 38] using the holographic model and in ref. [25] using the Nambu-Jona-Lasinio model. Further, the impact of vorticity on the dilepton production rate was investigated in ref. [39], where it was reported that the dilepton yield gets suppressed due to the presence of vorticity and the degree of suppression depends on the initial value of vorticity. The effect of magnetic field on different properties of the thermal QCD medium has been extensively studied using different methods [40–62], while the effect of rotation attracts growing interests recently. However, studies on the thermodynamic and transport properties of fast rotating QGP medium are still relatively few in the literature.

In this work, we intend to study the transport properties related to charge and heat, and some associated observables for the QGP medium subjected to the extreme conditions of rapid rotation and high temperature. It would be interesting to see how the rapid rotation modulates the flow of charge and heat in QGP medium. In addition, the observables, such as the Knudsen number, elliptic flow, specific heat at constant pressure, specific heat at constant volume, trace anomaly, thermal diffusion constant and isothermal compressibility are also most likely to be affected by the rotation of the QGP medium.

Consequently, it can be expected that this study on the transport phenomena and observables of QGP medium with rotation will provide deeper insight into the properties of the strongly interacting system. We determine the transport coefficients, such as the electrical conductivity and the thermal conductivity using the relativistic Boltzmann transport equation in the novel relaxation time approximation within the kinetic theory approach. The relaxation time approximation may defy the local particle number conservation in the medium, because the charge is not conserved instantaneously but only on the average basis over a cycle. However, the validity of the conservation laws can be satisfied by using the novel relaxation time approximation. In this method, the collision integral takes a modified form to ensure the validity of the energy-momentum conservation laws [63, 64]. Thus the novel relaxation time approximation preserves the fundamental properties of the collision associated with the microscopic conservation laws and is imperative when considering the momentum-dependent relaxation time. In addition, the rotational effect is incorporated through the parton distribution functions. Further, the interactions among partons are included through their thermal masses in the quasiparticle model. In this model, the quark-gluon plasma is treated as a medium consisting of thermally massive quasiparticles.

The present paper is organized as follows. In section 2, the electrical and thermal conductivities of a rotating QGP medium are studied by calculating them using the relativistic Boltzmann transport equation in the novel relaxation time approximation within the kinetic theory approach. The effects of rotation on the observables, such as the Knudsen number, elliptic flow, specific heat at constant pressure, specific heat at constant volume, trace anomaly, thermal diffusion constant and isothermal compressibility are also studied. The results on the aforesaid conductivities and observables are discussed in section 3. In section 4, the results of this work are concluded.

2 Rotating QGP medium

The emergence of rotation in a system could affect its various properties including the transport properties. In ref. [65], the phase-space distribution function for a relativistic rotating gas consisting of massive particles with spin S in the Boltzmann limit had been formulated. It can be generalized to the case of rotating QGP medium consisting of thermally massive quarks and gluons within the quasiparticle model (outside the quasiparticle model, *i.e.* with bare masses, the generalization might not be valid). The generalization of the distribution functions within the quasiparticle model is plausible, because it is well-known that, in the high temperature QCD regime, the thermally massive quark and gluon distribution functions can be approximated to the Boltzmann distributions. Thus, in a

rotating QGP medium, the phase-space distribution functions of partons get significantly affected. In such rotating system with angular velocity ω , the density operator can be written as

$$\hat{\rho} = \frac{1}{Z} e^{\beta(-\hat{H} + \mu\hat{N} + \omega\hat{J})} P_V, \quad (1)$$

where \hat{H} , \hat{N} and \hat{J} represent the Hamiltonian operator, the number operator and the angular momentum operator, respectively. Here, $T = \beta^{-1}$ and P_V denotes the projector onto the localized states $|h_V\rangle$, *i.e.* $P_V = \sum_{h_V} |h_V\rangle\langle h_V|$, which forms a complete set of quantum states for the system in a finite region V . The partition function, Z of the rotating system is expressed as

$$Z = \text{Tr} \left[e^{\beta(-\hat{H} + \mu\hat{N} + \omega\hat{J})} P_V \right]. \quad (2)$$

In the Boltzmann limit, it is possible to write the partition function (2) in terms of a product of the single particle partition functions. Thus, eq. (2) can be determined by computing the matrix elements of operators \hat{h} , \hat{n} and \hat{j} , suitable for single particles [65] as

$$\langle p, \tau | e^{\beta(-\hat{h} + \mu\hat{n} + \omega\hat{j})} P_V | p, \sigma \rangle = (e^{\beta(u_\mu p^\mu + a)} + b)^{-1} \langle p, \tau | e^{\beta\omega\hat{j}} P_V | p, \sigma \rangle, \quad (3)$$

where $a = -\mu$, $+\mu$ and 0 for quarks, antiquarks and gluons, respectively, and $b = +1$ for quarks as well as for antiquarks and $b = -1$ for gluons. In the above equation, τ and σ represent the polarization states. The matrix element appearing on the right-hand side of eq. (3) can be determined by the analytical continuation to the imaginary ω values. In this process, $\beta\omega$ is replaced by $-i\phi$ through the rotation $R_{\hat{\omega}}(\phi)$ around the axis ω by an angle ϕ . Now, the matrix element on the right-hand side of eq. (3) can be expanded [65] as

$$\begin{aligned} \langle p, \tau | e^{\beta\omega\hat{j}} P_V | p, \sigma \rangle &= \langle p, \tau | R_{\hat{\omega}}(\phi) P_V | p, \sigma \rangle \\ &= \sum_{\sigma'} \int d^3p' \langle p, \tau | R_{\hat{\omega}}(\phi) | p', \sigma' \rangle \langle p', \sigma' | P_V | p, \sigma \rangle. \end{aligned} \quad (4)$$

The matrix element of the representation of a rotation involves a Dirac delta function and a Wigner rotation matrix, *i.e.*,

$$\langle p, \tau | R_{\hat{\omega}}(\phi) | p', \sigma' \rangle = \delta^3(p - R_{\hat{\omega}}(\phi)(p')) D^S \left([R_{\hat{\omega}}(\phi)(p')]^{-1} R_{\hat{\omega}}(\phi) [p'] \right)_{\tau\sigma'}. \quad (5)$$

The matrix element of the projector P_V can be obtained by using the quantum field theoretical framework [66] as

$$\langle p', \sigma' | P_V | p, \sigma \rangle = \frac{1}{2} \sqrt{\frac{\varepsilon}{\varepsilon'}} \int d^3x e^{i\mathbf{x}\cdot(\mathbf{p}-\mathbf{p}')} \left(D^S \left([p']^{-1} [p] \right) + D^S \left([p']^\dagger [p]^\dagger^{-1} \right) \right)_{\sigma'\sigma} \langle 0 | P_V | 0 \rangle, \quad (6)$$

where $\langle 0|P_V|0\rangle$ is the vacuum expectation value of the projector P_V . For large volume V , $\langle 0|P_V|0\rangle \rightarrow 1$, because P_V tends to unity in this case. Substituting eq. (5) and eq. (6) in eq. (4), we have

$$\begin{aligned} \langle p, \tau | R_{\hat{\omega}}(\phi) P_V | p, \sigma \rangle &= \int d^3\mathbf{x} e^{i\mathbf{x}\cdot(\mathbf{p}-R_{\hat{\omega}}(\phi)^{-1}(\mathbf{p}))} \\ &\times \frac{1}{2} \left(D^S([p]^{-1} R_{\hat{\omega}}(\phi) [p]) + D^S([p]^\dagger R_{\hat{\omega}}(\phi) [p]^{\dagger-1}) \right)_{\tau\sigma}. \end{aligned} \quad (7)$$

Using the unitarity of the Wigner rotation, *i.e.*,

$$D^S\left([R_{\hat{\omega}}(\phi)(p')]^{-1} R_{\hat{\omega}}(\phi) [p']\right) = D^S\left([R_{\hat{\omega}}(\phi)(p')]^\dagger R_{\hat{\omega}}(\phi) [p']^{\dagger-1}\right),$$

eq. (7) can be analytically extended to the imaginary angles. Thus the matrix element in eq. (3) takes the following form,

$$\begin{aligned} \langle p, \tau | e^{\beta\omega\hat{j}} P_V | p, \sigma \rangle &= \int d^3\mathbf{x} e^{i\mathbf{x}\cdot(\mathbf{p}-R_{\hat{\omega}}(i\beta\omega)^{-1}(\mathbf{p}))} \\ &\times \frac{1}{2} \left(D^S([p]^{-1} R_{\hat{\omega}}(i\beta\omega) [p]) + D^S([p]^\dagger R_{\hat{\omega}}(i\beta\omega) [p]^{\dagger-1}) \right)_{\tau\sigma}. \end{aligned} \quad (8)$$

It can be observed that, $R_{\hat{\omega}}(i\beta\omega) = e^{\beta\omega\hat{j}}$. The matrix element in eq. (3) has a spatial integral form, which allows us to write the phase-space distribution function [65] as

$$\begin{aligned} f(x, p)_{\tau\sigma} &= (e^{\beta(u_\mu p^\mu + a)} + b)^{-1} e^{i\mathbf{x}\cdot(\mathbf{p}-R_{\hat{\omega}}(i\beta\omega)^{-1}(\mathbf{p}))} \\ &\times \frac{1}{2} \left(D^S([p]^{-1} R_{\hat{\omega}}(i\beta\omega) [p]) + D^S([p]^\dagger R_{\hat{\omega}}(i\beta\omega) [p]^{\dagger-1}) \right)_{\tau\sigma}, \end{aligned} \quad (9)$$

where u_μ accounts for the four-velocity of fluid. For high temperature QCD medium, $\beta\omega$ is small, *i.e.* $\beta\omega < 1$. Thus the difference between momenta in the exponent of eq. (9) can be approximated by the lowest order term in $\beta\omega$,

$$\begin{aligned} \mathbf{p} - R_{\hat{\omega}}(i\beta\omega)^{-1}(\mathbf{p}) &= \mathbf{p} - [(\cosh \beta\omega) \mathbf{p} - i(\sinh \beta\omega) \hat{\omega} \times \mathbf{p} + (1 - \cosh \beta\omega) \mathbf{p} \hat{\omega} \hat{\omega}] \\ &\simeq i\beta \boldsymbol{\omega} \times \mathbf{p}. \end{aligned} \quad (10)$$

Now, the phase-space distribution function becomes

$$\begin{aligned} f(x, p)_{\tau\sigma} &= (e^{\beta(u_\mu p^\mu + a)} + b)^{-1} e^{-\beta\mathbf{x}\cdot(\boldsymbol{\omega} \times \mathbf{p})} \\ &\times \frac{1}{2} \left(D^S([p]^{-1} R_{\hat{\omega}}(i\beta\omega) [p]) + D^S([p]^\dagger R_{\hat{\omega}}(i\beta\omega) [p]^{\dagger-1}) \right)_{\tau\sigma} \\ &= (e^{\beta(u_\mu p^\mu + a)} + b)^{-1} e^{\beta\mathbf{p}\cdot\mathbf{v}} \\ &\times \frac{1}{2} \left(D^S([p]^{-1} R_{\hat{\omega}}(i\beta\omega) [p]) + D^S([p]^\dagger R_{\hat{\omega}}(i\beta\omega) [p]^{\dagger-1}) \right)_{\tau\sigma}, \end{aligned} \quad (11)$$

where $\mathbf{v} = \boldsymbol{\omega} \times \mathbf{x}$ has been used. The above equation is the unnormalized single-particle phase-space distribution function. By taking the trace of the matrix (11), one can obtain

the phase-space density in (x, p) as

$$\begin{aligned} f(x, p) &= \sum_{\sigma} f(x, p)_{\sigma\sigma} \\ &= (e^{\beta(u_{\mu}p^{\mu}+a)} + b)^{-1} e^{\beta\mathbf{p}\cdot\mathbf{v}} \chi(\beta\omega). \end{aligned} \quad (12)$$

In the local rest frame, $\mathbf{v} = 0$. So, we have

$$f(x, p) = \frac{1}{e^{\beta(u_{\mu}p^{\mu}+a)} + b} \chi(\beta\omega), \quad (13)$$

where $\chi(\beta\omega)$ represents the angular velocity-dependent part and is given by

$$\begin{aligned} \chi(\beta\omega) &= \text{Tr} [D^S (R_{\hat{\omega}}(i\beta\omega))] \\ &= \frac{\sinh((S + \frac{1}{2})\beta\omega)}{\sinh(\frac{\beta\omega}{2})}. \end{aligned} \quad (14)$$

For quarks and antiquarks, spin $S = \frac{1}{2}$ and for gluons, $S = 1$. Accordingly, they have different expressions for $\chi(\beta\omega)$ and hence, they have different forms of the distribution functions. Thus the quark, antiquark and gluon distribution functions at finite rotation can be written as

$$f_q = f_0^q \chi_q(\beta\omega), \quad (15)$$

$$\bar{f}_q = \bar{f}_0^q \chi_{\bar{q}}(\beta\omega), \quad (16)$$

$$f_g = f_0^g \chi_g(\beta\omega), \quad (17)$$

respectively. The quantities in the above equations are defined as follows,

$$\begin{aligned} f_0^q &= \frac{1}{e^{\beta(u_{\mu}p^{\mu}-\mu)} + 1} = \frac{1}{e^{\beta(\omega_f-\mu)} + 1}, \quad \bar{f}_0^q = \frac{1}{e^{\beta(u_{\mu}p^{\mu}+\mu)} + 1} = \frac{1}{e^{\beta(\omega_f+\mu)} + 1}, \\ f_0^g &= \frac{1}{e^{\beta u_{\mu}p^{\mu}} - 1} = \frac{1}{e^{\beta\omega_g} - 1}, \quad \chi_q(\beta\omega) = \frac{\sinh(\beta\omega)}{\sinh(\beta\omega/2)}, \\ \chi_{\bar{q}}(\beta\omega) &= \frac{\sinh(\beta\omega)}{\sinh(\beta\omega/2)}, \quad \chi_g(\beta\omega) = \frac{\sinh(3\beta\omega/2)}{\sinh(\beta\omega/2)}, \end{aligned}$$

where ω_f is the energy of the f th flavor of quark (antiquark) and ω_g is the energy of the gluon in the rotating QGP medium. We note that the flavor degrees of freedom are taken into account explicitly. Further, the chemical potentials for flavors, u , d and s are kept the same ($\mu_f = \mu$).

2.1 Charge conduction in rotating QGP medium

When a rotating QGP medium is exposed to an external electric field, an electric current gets induced and the corresponding four-current density is written as

$$J^{\mu} = \sum_f g_f \int \frac{d^3\mathbf{p}}{(2\pi)^3 \omega_f} p^{\mu} [q_f \delta f_q + \bar{q}_f \delta \bar{f}_q], \quad (18)$$

where g_f , q_f (\bar{q}_f) and δf_q ($\delta \bar{f}_q$) represent the degeneracy factor, electric charge and infinitesimal change in the quark (antiquark) distribution function of f th flavor, respectively. According to Ohm's law, the spatial component of four-current density is directly proportional to the external electric field with the proportionality factor being the electrical conductivity (σ_{el}), *i.e.*,

$$\mathbf{J} = \sigma_{\text{el}} \mathbf{E} . \quad (19)$$

In order to calculate the infinitesimal change δf_q , we use the relativistic Boltzmann transport equation (RBTE) in the novel relaxation time approximation (RTA). In this approximation, the collision integral takes a modified form for the validity of the conservation laws [63, 64]. However, in the frequently used relaxation time approximation, the conservation laws are satisfied, if the relaxation time is momentum-independent. The RBTE in the novel RTA is written as

$$p^\mu \frac{\partial f'_q}{\partial x^\mu} + q_f F^{\rho\sigma} p_\sigma \frac{\partial f'_q}{\partial p^\rho} = -\frac{p_\nu u^\nu}{\tau_f} \left[\delta f_q - \frac{\langle (\omega_f/\tau_f) \delta f_q \rangle_0}{\langle \omega_f/\tau_f \rangle_0} + \frac{P_1^{(0)} \langle (\omega_f/\tau_f) P_1^{(0)} \delta f_q \rangle_0}{\langle (\omega_f/\tau_f) P_1^{(0)} P_1^{(0)} \rangle_0} + \frac{p^{\langle \mu \rangle} \langle (\omega_f/\tau_f) p_{\langle \mu \rangle} \delta f_q \rangle_0}{(1/3) \langle (\omega_f/\tau_f) p_{\langle \mu \rangle} p^{\langle \mu \rangle} \rangle_0} \right], \quad (20)$$

where τ_f represents the novel relaxation time, $f'_q = \delta f_q + f_q$ with δf_q denoting the infinitesimal change of the quark distribution function due to the external field and $F^{\rho\sigma}$ is the electromagnetic field strength tensor, whose components are related to the electric and magnetic fields. The novel relaxation time for quarks (antiquarks), τ_f ($\tau_{\bar{f}}$) is momentum-dependent with the following form,

$$\tau_{f(\bar{f})} = (\beta\omega_f)^\xi t_{f(\bar{f})}, \quad (21)$$

where ξ is an arbitrary constant that controls the energy dependence of the relaxation time and $t_{f(\bar{f})}$ is momentum-independent, whose form is given [67] by

$$t_{f(\bar{f})} = \frac{1}{5.1T\alpha_s^2 \log(1/\alpha_s) [1 + 0.12(2N_f + 1)]}. \quad (22)$$

For the calculations, the value of ξ can be taken up to 1, for example, in QCD kinetic theories, $\xi = \frac{1}{2}$ [68], while in scalar field theories $\xi = 1$ [69].

In eq. (20), $P_1^{(0)}$ and $p^{\langle \mu \rangle}$ are respectively defined as

$$P_1^{(0)} = 1 - \frac{\langle \omega_f/\tau_f \rangle_0 \omega_f}{\langle \omega_f^2/\tau_f \rangle_0}, \quad (23)$$

$$p^{\langle \mu \rangle} = \Delta^{\mu\nu} p_\nu, \quad (24)$$

where $\Delta^{\mu\nu} = g^{\mu\nu} - u^\mu u^\nu$. The momentum integral of A (A can be different terms appearing inside the angular brackets in eq. (20)) relative to the local equilibrium distribution

function is defined as

$$\langle A \rangle_0 = \int \frac{d^3\mathbf{p}}{(2\pi)^3 \omega_f} A f_q. \quad (25)$$

Using equations (23), (24), (25) and integration by parts, the second (say L^2), third (say L^3) and fourth (say L^4) terms appearing inside the square bracket of eq. (20) can be calculated to take the following forms,

$$L^2 = \delta f_q, \quad (26)$$

$$L^3 = \frac{\delta f_q \left(1 - \frac{\omega_f \int d\mathbf{p} \frac{\mathbf{p}^2 f_q}{\tau_f}}{\int d\mathbf{p} \frac{\mathbf{p}^2 \omega_f f_q}{\tau_f}} \right) \int d\mathbf{p} \frac{\mathbf{p}^2 f_q}{\tau_f} \left(1 - \frac{\omega_f \int d\mathbf{p} \frac{\mathbf{p}^2 f_q}{\tau_f}}{\int d\mathbf{p} \frac{\mathbf{p}^2 \omega_f f_q}{\tau_f}} \right)}{\int d\mathbf{p} \frac{\mathbf{p}^2 f_q}{\tau_f} \left(1 - \frac{\omega_f \int d\mathbf{p} \frac{\mathbf{p}^2 f_q}{\tau_f}}{\int d\mathbf{p} \frac{\mathbf{p}^2 \omega_f f_q}{\tau_f}} \right)^2}, \quad (27)$$

$$L^4 = \frac{3 \delta f_q \int d\mathbf{p} \frac{\mathbf{p}^3 f_q}{\tau_f}}{\int d\mathbf{p} \frac{\mathbf{p}^4 f_q}{\tau_f}}. \quad (28)$$

For the calculation of electrical conductivity, we use the components of $F^{\rho\sigma}$ associated with only electric field. Moreover, in case of a spatially homogeneous distribution function with the steady-state condition, we use $\frac{\partial f'_q}{\partial \mathbf{r}} = 0$ and $\frac{\partial f'_q}{\partial t} = 0$. Thus, RBTE (20) becomes

$$q_f \mathbf{E} \cdot \mathbf{p} \frac{\partial f'_q}{\partial p_0} + q_f p_0 \mathbf{E} \cdot \frac{\partial f'_q}{\partial \mathbf{p}} = -\frac{p_0}{\tau_f} \delta f_q J, \quad (29)$$

where the expression of J is written as

$$J = \frac{\left(1 - \frac{\omega_f \int d\mathbf{p} \frac{\mathbf{p}^2 f_q}{\tau_f}}{\int d\mathbf{p} \frac{\mathbf{p}^2 \omega_f f_q}{\tau_f}} \right) \int d\mathbf{p} \frac{\mathbf{p}^2 f_q}{\tau_f} \left(1 - \frac{\omega_f \int d\mathbf{p} \frac{\mathbf{p}^2 f_q}{\tau_f}}{\int d\mathbf{p} \frac{\mathbf{p}^2 \omega_f f_q}{\tau_f}} \right)}{\int d\mathbf{p} \frac{\mathbf{p}^2 f_q}{\tau_f} \left(1 - \frac{\omega_f \int d\mathbf{p} \frac{\mathbf{p}^2 f_q}{\tau_f}}{\int d\mathbf{p} \frac{\mathbf{p}^2 \omega_f f_q}{\tau_f}} \right)^2} + \frac{3p \int d\mathbf{p} \frac{\mathbf{p}^3 f_q}{\tau_f}}{\int d\mathbf{p} \frac{\mathbf{p}^4 f_q}{\tau_f}}. \quad (30)$$

In the antiquark case, \bar{J} is given by

$$\bar{J} = \frac{\left(1 - \frac{\omega_f \int d\mathbf{p} \frac{\mathbf{p}^2 \bar{f}_q}{\tau_{\bar{f}}}}{\int d\mathbf{p} \frac{\mathbf{p}^2 \omega_f \bar{f}_q}{\tau_{\bar{f}}}} \right) \int d\mathbf{p} \frac{\mathbf{p}^2 \bar{f}_q}{\tau_{\bar{f}}} \left(1 - \frac{\omega_f \int d\mathbf{p} \frac{\mathbf{p}^2 \bar{f}_q}{\tau_{\bar{f}}}}{\int d\mathbf{p} \frac{\mathbf{p}^2 \omega_f \bar{f}_q}{\tau_{\bar{f}}}} \right)}{\int d\mathbf{p} \frac{\mathbf{p}^2 \bar{f}_q}{\tau_{\bar{f}}} \left(1 - \frac{\omega_f \int d\mathbf{p} \frac{\mathbf{p}^2 \bar{f}_q}{\tau_{\bar{f}}}}{\int d\mathbf{p} \frac{\mathbf{p}^2 \omega_f \bar{f}_q}{\tau_{\bar{f}}}} \right)^2} + \frac{3p \int d\mathbf{p} \frac{\mathbf{p}^3 \bar{f}_q}{\tau_{\bar{f}}}}{\int d\mathbf{p} \frac{\mathbf{p}^4 \bar{f}_q}{\tau_{\bar{f}}}}. \quad (31)$$

Using equations (15), (16) and (21) in equations (30) and (31), both J and \bar{J} can be

simplified, and they are respectively written as

$$J = \frac{\left(1 - \frac{\omega_f \int d\mathbf{p} \frac{\mathbf{p}^2 f_0^q}{\omega_f^\xi}}{\int d\mathbf{p} \frac{\mathbf{p}^2 f_0^q}{\omega_f^{\xi-1}}}\right) \int d\mathbf{p} \frac{\mathbf{p}^2 f_0^q}{\omega_f^\xi} \left(1 - \frac{\omega_f \int d\mathbf{p} \frac{\mathbf{p}^2 f_0^q}{\omega_f^\xi}}{\int d\mathbf{p} \frac{\mathbf{p}^2 f_0^q}{\omega_f^{\xi-1}}}\right)}{\int d\mathbf{p} \frac{\mathbf{p}^2 f_0^q}{\omega_f^\xi} \left(1 - \frac{\omega_f \int d\mathbf{p} \frac{\mathbf{p}^2 f_0^q}{\omega_f^\xi}}{\int d\mathbf{p} \frac{\mathbf{p}^2 f_0^q}{\omega_f^{\xi-1}}}\right)^2} + \frac{3\mathbf{p} \int d\mathbf{p} \frac{\mathbf{p}^3 f_0^q}{\omega_f^\xi}}{\int d\mathbf{p} \frac{\mathbf{p}^4 f_0^q}{\omega_f^\xi}}, \quad (32)$$

$$\bar{J} = \frac{\left(1 - \frac{\omega_f \int d\mathbf{p} \frac{\mathbf{p}^2 \bar{f}_0^q}{\omega_f^\xi}}{\int d\mathbf{p} \frac{\mathbf{p}^2 \bar{f}_0^q}{\omega_f^{\xi-1}}}\right) \int d\mathbf{p} \frac{\mathbf{p}^2 \bar{f}_0^q}{\omega_f^\xi} \left(1 - \frac{\omega_f \int d\mathbf{p} \frac{\mathbf{p}^2 \bar{f}_0^q}{\omega_f^\xi}}{\int d\mathbf{p} \frac{\mathbf{p}^2 \bar{f}_0^q}{\omega_f^{\xi-1}}}\right)}{\int d\mathbf{p} \frac{\mathbf{p}^2 \bar{f}_0^q}{\omega_f^\xi} \left(1 - \frac{\omega_f \int d\mathbf{p} \frac{\mathbf{p}^2 \bar{f}_0^q}{\omega_f^\xi}}{\int d\mathbf{p} \frac{\mathbf{p}^2 \bar{f}_0^q}{\omega_f^{\xi-1}}}\right)^2} + \frac{3\mathbf{p} \int d\mathbf{p} \frac{\mathbf{p}^3 \bar{f}_0^q}{\omega_f^\xi}}{\int d\mathbf{p} \frac{\mathbf{p}^4 \bar{f}_0^q}{\omega_f^\xi}}. \quad (33)$$

From eq. (29), δf_q is obtained as

$$\delta f_q = \frac{2\tau_f q_f \beta}{\omega_f J} \mathbf{E} \cdot \mathbf{p} f_0^q (1 - f_0^q) \chi_q(\beta\omega). \quad (34)$$

Similarly, $\delta \bar{f}_q$ for antiquark is determined as

$$\delta \bar{f}_q = \frac{2\tau_{\bar{f}} \bar{q}_f \beta}{\omega_f \bar{J}} \mathbf{E} \cdot \mathbf{p} \bar{f}_0^q (1 - \bar{f}_0^q) \chi_{\bar{q}}(\beta\omega). \quad (35)$$

Substituting the values of δf_q and $\delta \bar{f}_q$ in eq. (18), using eq. (21) and then comparing with eq. (19), we get the electrical conductivity for a rotating QGP medium as

$$\sigma_{\text{el}} = \frac{\beta^{1+\xi}}{3\pi^2} \sum_f g_f q_f^2 \int d\mathbf{p} \frac{\mathbf{p}^4}{\omega_f^{2-\xi}} \left[\frac{t_f}{J} f_0^q (1 - f_0^q) \chi_q(\beta\omega) + \frac{t_{\bar{f}}}{\bar{J}} \bar{f}_0^q (1 - \bar{f}_0^q) \chi_{\bar{q}}(\beta\omega) \right]. \quad (36)$$

2.2 Heat conduction in rotating QGP medium

In a thermal medium, the heat flow four-vector is related to the energy diffusion and the enthalpy diffusion as

$$Q_\mu = \Delta_{\mu\alpha} T^{\alpha\beta} u_\beta - h \Delta_{\mu\alpha} N^\alpha, \quad (37)$$

where $T^{\alpha\beta}$ is the energy-momentum tensor, N^α represents the particle flow four-vector, $\Delta_{\mu\alpha} = g_{\mu\alpha} - u_\mu u_\alpha$, the enthalpy per particle $h = (\varepsilon + P)/n$ with ε , P and n denoting the energy density, the pressure and the particle number density, respectively. N^α and $T^{\alpha\beta}$ are also known as the first and second moments of the distribution function, respectively

with the following expressions,

$$N^\alpha = \sum_f g_f \int \frac{d^3\mathbf{p}}{(2\pi)^3 \omega_f} p^\alpha [f_q + \bar{f}_q], \quad (38)$$

$$T^{\alpha\beta} = \sum_f g_f \int \frac{d^3\mathbf{p}}{(2\pi)^3 \omega_f} p^\alpha p^\beta [f_q + \bar{f}_q]. \quad (39)$$

Using N^α and $T^{\alpha\beta}$, it is possible to get $n = N^\alpha u_\alpha$, $\varepsilon = u_\alpha T^{\alpha\beta} u_\beta$ and $P = -\Delta_{\alpha\beta} T^{\alpha\beta} / 3$. In the local rest frame, the heat flow is purely spatial, because $Q_\mu u^\mu = 0$. Hence, the spatial component of the heat flow remains finite and is expressed as

$$Q^i = \sum_f g_f \int \frac{d^3\mathbf{p}}{(2\pi)^3} \frac{p^i}{\omega_f} [(\omega_f - h_f) \delta f_q + (\omega_f - \bar{h}_f) \delta \bar{f}_q]. \quad (40)$$

The Navier-Stokes equation relates the heat flow with the gradients of temperature and pressure as

$$Q^i = -\kappa \delta^{ij} \left[\partial_j T - \frac{T}{\varepsilon + P} \partial_j P \right], \quad (41)$$

where κ is the thermal conductivity. For the calculation of thermal conductivity, the electromagnetic field strength part is not required, so it can be dropped from the relativistic Boltzmann transport equation (20). Now, expanding the gradient of the particle distribution function in terms of the gradients of the flow velocity and the temperature in the novel relaxation time approximation, we have

$$\begin{aligned} -p^\mu f_0^q (1 - f_0^q) \chi_q(\beta\omega) [(u_\alpha p^\alpha) \partial_\mu \beta + \beta \partial_\mu (u_\alpha p^\alpha) - \partial_\mu (\beta\mu)] + p^\mu f_0^q \partial_\mu (\chi_q(\beta\omega)) = -\frac{p_\nu u^\nu}{\tau_f} [\delta f_q \\ - \frac{\langle (\omega_f / \tau_f) \delta f_q \rangle_0}{\langle \omega_f / \tau_f \rangle_0} + \frac{P_1^{(0)} \langle (\omega_f / \tau_f) P_1^{(0)} \delta f_q \rangle_0}{\langle (\omega_f / \tau_f) P_1^{(0)} P_1^{(0)} \rangle_0} + \frac{p^{(\mu)} \langle (\omega_f / \tau_f) p_{(\mu)} \delta f_q \rangle_0}{(1/3) \langle (\omega_f / \tau_f) p_{(\mu)} p^{(\mu)} \rangle_0}] \end{aligned} \quad (42)$$

After solving eq. (42), δf_q can be obtained as

$$\begin{aligned} \delta f_q = & -\frac{\beta \tau_f f_0^q (1 - f_0^q)}{J} \chi_q(\beta\omega) \left[\frac{(\omega_f - h_f) p^j}{T \omega_f} \left(\partial_j T - \frac{T}{n h_f} \partial_j P \right) + p_0 \frac{DT}{T} - \frac{p^\mu p^\alpha}{p_0} \nabla_\mu u_\alpha \right. \\ & \left. + TD \left(\frac{\mu}{T} \right) \right] - \frac{\beta \tau_f f_0^q}{J} \sinh \left(\frac{\beta\omega}{2} \right) \left[TD \left(\frac{\omega}{T} \right) + \frac{T p^\alpha}{p_0} \nabla_\alpha \left(\frac{\omega}{T} \right) \right]. \end{aligned} \quad (43)$$

In the similar way, $\delta \bar{f}_q$ for antiquark is determined as

$$\begin{aligned} \delta \bar{f}_q = & -\frac{\beta \tau_{\bar{f}} \bar{f}_0^q (1 - \bar{f}_0^q)}{\bar{J}} \chi_{\bar{q}}(\beta\omega) \left[\frac{(\omega_f - \bar{h}_f) p^j}{T \omega_f} \left(\partial_j T - \frac{T}{n \bar{h}_f} \partial_j P \right) + p_0 \frac{DT}{T} - \frac{p^\mu p^\alpha}{p_0} \nabla_\mu u_\alpha \right. \\ & \left. - TD \left(\frac{\mu}{T} \right) \right] - \frac{\beta \tau_{\bar{f}} \bar{f}_0^q}{\bar{J}} \sinh \left(\frac{\beta\omega}{2} \right) \left[TD \left(\frac{\omega}{T} \right) + \frac{T p^\alpha}{p_0} \nabla_\alpha \left(\frac{\omega}{T} \right) \right]. \end{aligned} \quad (44)$$

Substituting the values of δf_q and $\delta \bar{f}_q$ in eq. (40), using eq. (21) and then comparing with eq. (41), we get the thermal conductivity for a rotating QGP medium as

$$\begin{aligned} \kappa = & \frac{\beta^{2+\xi}}{6\pi^2} \sum_f g_f \int d\mathbf{p} \frac{p^4}{\omega_f^{2-\xi}} \left[\frac{t_f}{J} (\omega_f - h_f)^2 f_0^q (1 - f_0^q) \chi_q(\beta\omega) \right. \\ & \left. + \frac{t_{\bar{f}}}{J} (\omega_f - \bar{h}_f)^2 \bar{f}_0^q (1 - \bar{f}_0^q) \chi_{\bar{q}}(\beta\omega) \right]. \end{aligned} \quad (45)$$

2.3 Observables in rotating QGP medium

The observables such as the Knudsen number, the elliptic flow, the specific heat at constant pressure, the specific heat at constant volume, the trace anomaly, the thermal diffusion constant and the isothermal compressibility are also likely to be affected by the rotation of the QGP medium.

The Knudsen number is the ratio of the mean free path (λ) to the characteristic length scale (l) of the medium, *i.e.* $\Omega = \lambda/l$. For the medium to be in the equilibrium state, l should be larger than λ . Using $\lambda = 3\kappa/(vC_V)$, the Knudsen number becomes

$$\Omega = \frac{3\kappa}{lvC_V}, \quad (46)$$

where v and C_V are the relative speed and the specific heat at constant volume, respectively. The Knudsen number explains the competition between the microscopic and macroscopic length scales of the concerned system. If Ω is less than unity, then the equilibrium hydrodynamics can be applicable and in the hydrodynamic limit, the system assumes local thermodynamical equilibrium. On the other hand, the Knudsen number is large for rarefied gases and the regime of extremely large Ω is known as the free streaming particle regime. In heavy ion collisions, the degree of thermalization in the produced matter can be characterized by the Knudsen number. The experimental extraction of the Knudsen number may rely on various quantities, such as the overlap area between two colliding nuclei in the transverse plane of the collision zone, eccentricity, multiplicity density, centrality etc. It is reported in ref. [70] that the inverse of the Knudsen number can be obtained experimentally as it is directly proportional to the multiplicity density and inversely proportional to the transverse area of the collision zone. In this work, we have used $v \simeq 1$ and $l = 1$ fm, and calculated C_V from the energy-momentum tensor as

follows,

$$\begin{aligned}
C_V &= \frac{\partial(u_\mu T^{\mu\nu} u_\nu)}{\partial T} \\
&= \sum_f g_f \int \frac{d^3\mathbf{p}}{(2\pi)^3} \omega_f \left[\frac{\partial f_q}{\partial T} + \frac{\partial \bar{f}_q}{\partial T} \right] + g_g \int \frac{d^3\mathbf{p}}{(2\pi)^3} \omega_g \frac{\partial f_g}{\partial T} \\
&= \frac{1}{2\pi^2} \sum_f g_f \int d\mathbf{p} p^2 \omega_f \left[\chi_q(\beta\omega) \frac{\partial f_0^q}{\partial T} + f_0^q \frac{\partial \chi_q(\beta\omega)}{\partial T} + \chi_{\bar{q}}(\beta\omega) \frac{\partial \bar{f}_0^q}{\partial T} + \bar{f}_0^q \frac{\partial \chi_{\bar{q}}(\beta\omega)}{\partial T} \right] \\
&\quad + \frac{1}{2\pi^2} g_g \int d\mathbf{p} p^2 \omega_g \left[\chi_g(\beta\omega) \frac{\partial f_0^g}{\partial T} + f_0^g \frac{\partial \chi_g(\beta\omega)}{\partial T} \right]. \tag{47}
\end{aligned}$$

In the above equation, the values of different partial derivatives are given by

$$\frac{\partial f_0^q}{\partial T} = \beta^2 (\omega_f - \mu) f_0^q (1 - f_0^q), \tag{48}$$

$$\frac{\partial \bar{f}_0^q}{\partial T} = \beta^2 (\omega_f + \mu) \bar{f}_0^q (1 - \bar{f}_0^q), \tag{49}$$

$$\frac{\partial f_0^g}{\partial T} = \beta^2 \omega_g f_0^g (1 + f_0^g), \tag{50}$$

$$\frac{\partial \chi_q(\beta\omega)}{\partial T} = \frac{\partial \chi_{\bar{q}}(\beta\omega)}{\partial T} = -\beta^2 \omega \sinh\left(\frac{\beta\omega}{2}\right), \tag{51}$$

$$\frac{\partial \chi_g(\beta\omega)}{\partial T} = -2\beta^2 \omega \sinh(\beta\omega). \tag{52}$$

Now, eq. (47) becomes

$$\begin{aligned}
C_V &= \frac{\beta^2}{2\pi^2} \sum_f g_f \int d\mathbf{p} p^2 \omega_f \left[\{(\omega_f - \mu) f_0^q (1 - f_0^q) + (\omega_f + \mu) \bar{f}_0^q (1 - \bar{f}_0^q)\} \frac{\sinh(\beta\omega)}{\sinh(\beta\omega/2)} \right. \\
&\quad \left. - (f_0^q + \bar{f}_0^q) \omega \sinh(\beta\omega/2) \right] + \frac{\beta^2}{2\pi^2} g_g \int d\mathbf{p} p^2 \omega_g \left[\omega_g f_0^g (1 + f_0^g) \frac{\sinh(3\beta\omega/2)}{\sinh(\beta\omega/2)} \right. \\
&\quad \left. - 2f_0^g \omega \sinh(\beta\omega) \right]. \tag{53}
\end{aligned}$$

Using the values of κ (45) and C_V (53) in eq. (46), the Knudsen number for the QGP medium at finite rotation can be explored.

The elliptic flow (v_2) is one of the key observables and represents the azimuthal anisotropy in the production of particles in ultrarelativistic heavy ion collisions at terrestrial laboratories. In such collisions, the overlapping region of bombarding nuclei is the origin of generation of the elliptic flow, where the pressure gradient converts the initial spatial anisotropy (quantified by the eccentricity ϵ) into the momentum anisotropy. The elliptic flow develops gradually with the evolution of the system. The anisotropy of the momentum distributions can be completely attained only once all parts of the system get involved in the process. It also gives the information about the degree of interactions/reinteractions among the particles produced in heavy ion collisions. Thus,

its magnitude is associated with the equilibrium property of the thermal medium and any deviation from equilibrium can reduce the magnitude of such flow. Experimentally, elliptic flow can be analyzed by selecting events in a centrality class. The quantities which influence the elliptic flow, such as the density, the transverse size and the eccentricity, fluctuate from one event to the other, thus causing dynamical fluctuations of the elliptic flow. The elliptic flow is closely related to the Knudsen number and is defined [70–72] as

$$v_2 = \frac{v_2^h}{1 + \frac{\Omega}{\Omega_h}}. \quad (54)$$

Here, v_2^h denotes the elliptic flow in the hydrodynamic limit ($\Omega \rightarrow 0$ limit) and Ω_h is the value of the Knudsen number calculated by observing the transition between the hydrodynamic regime and the free streaming particle regime. The transport calculation [72] has estimated $\Omega_h \approx 0.7$ and $v_2^h \approx 0.1$. The presence of magnetic field, temperature and chemical potential were observed to influence the elliptic flow [46, 73, 74]. Similarly, the finite rotation could also affect the elliptic flow. Substituting the value of Ω (46) in eq. (54), the effect of finite rotation on the elliptic flow can be investigated.

Like the specific heat at constant volume, it is possible to determine the specific heat at constant pressure from the energy-momentum tensor as

$$\begin{aligned} C_P &= \frac{\partial(u_\mu T^{\mu\nu} u_\nu - \Delta_{\mu\nu} T^{\mu\nu}/3)}{\partial T} \\ &= \sum_f g_f \int \frac{d^3\mathbf{p}}{(2\pi)^3} \omega_f \left[\frac{\partial f_q}{\partial T} + \frac{\partial \bar{f}_q}{\partial T} \right] + \frac{1}{3} \sum_f g_f \int \frac{d^3\mathbf{p}}{(2\pi)^3} \frac{p^2}{\omega_f} \left[\frac{\partial f_q}{\partial T} + \frac{\partial \bar{f}_q}{\partial T} \right] \\ &\quad + g_g \int \frac{d^3\mathbf{p}}{(2\pi)^3} \omega_g \frac{\partial f_g}{\partial T} + \frac{1}{3} g_g \int \frac{d^3\mathbf{p}}{(2\pi)^3} \frac{p^2}{\omega_g} \frac{\partial f_g}{\partial T} \\ &= \frac{1}{2\pi^2} \sum_f g_f \int d\mathbf{p} p^2 \omega_f \left[\chi_q(\beta\omega) \frac{\partial f_0^q}{\partial T} + f_0^q \frac{\partial \chi_q(\beta\omega)}{\partial T} + \chi_{\bar{q}}(\beta\omega) \frac{\partial \bar{f}_0^q}{\partial T} + \bar{f}_0^q \frac{\partial \chi_{\bar{q}}(\beta\omega)}{\partial T} \right] \\ &\quad + \frac{1}{6\pi^2} \sum_f g_f \int d\mathbf{p} \frac{p^4}{\omega_f} \left[\chi_q(\beta\omega) \frac{\partial f_0^q}{\partial T} + f_0^q \frac{\partial \chi_q(\beta\omega)}{\partial T} + \chi_{\bar{q}}(\beta\omega) \frac{\partial \bar{f}_0^q}{\partial T} + \bar{f}_0^q \frac{\partial \chi_{\bar{q}}(\beta\omega)}{\partial T} \right] \\ &\quad + \frac{1}{2\pi^2} g_g \int d\mathbf{p} p^2 \omega_g \left[\chi_g(\beta\omega) \frac{\partial f_0^g}{\partial T} + f_0^g \frac{\partial \chi_g(\beta\omega)}{\partial T} \right] \\ &\quad + \frac{1}{6\pi^2} g_g \int d\mathbf{p} \frac{p^4}{\omega_g} \left[\chi_g(\beta\omega) \frac{\partial f_0^g}{\partial T} + f_0^g \frac{\partial \chi_g(\beta\omega)}{\partial T} \right]. \quad (55) \end{aligned}$$

Substituting the values of partial derivatives in the above equation and simplifying, we

get

$$\begin{aligned}
C_P = & \frac{\beta^2}{6\pi^2} \sum_f g_f \int d\mathbf{p} \left(3\mathbf{p}^2 \omega_f + \frac{\mathbf{p}^4}{\omega_f} \right) \left[\{ (\omega_f - \mu) f_0^q (1 - f_0^q) + (\omega_f + \mu) \bar{f}_0^q (1 - \bar{f}_0^q) \} \right. \\
& \times \left. \frac{\sinh(\beta\omega)}{\sinh(\beta\omega/2)} - (f_0^q + \bar{f}_0^q) \omega \sinh(\beta\omega/2) \right] \\
& + \frac{\beta^2}{6\pi^2} g_g \int d\mathbf{p} \left(3\mathbf{p}^2 \omega_g + \frac{\mathbf{p}^4}{\omega_g} \right) \left[\omega_g f_0^g (1 + f_0^g) \frac{\sinh(3\beta\omega/2)}{\sinh(\beta\omega/2)} - 2f_0^g \omega \sinh(\beta\omega) \right] \quad (56)
\end{aligned}$$

From C_P (56) and C_V (53), the adiabatic index can be determined and studied to understand the effect of rotation on it, which is defined as

$$\gamma = \frac{C_P}{C_V}. \quad (57)$$

This ratio measures how much internal energy is getting converted into work in any compression/expansion process. Different systems possess different γ values, *e.g.* for a nonrelativistic ideal gas, $\gamma = \frac{5}{3}$ and for a system with massless particles, $\gamma = \frac{4}{3}$. The adiabatic index for an ideal gas is also associated with the degrees of freedom, so, for monatomic, diatomic and triatomic gases, the values of γ are different. As C_P and C_V for the system of quarks, antiquarks and gluons are influenced by the extreme conditions, their ratio is supposed to change in such conditions. Thus the adiabatic index depends on the features of the medium and its physical conditions. Since the rotation significantly affects the properties of the QGP medium, the value of the adiabatic index must be affected.

The trace anomaly is also one of the important thermodynamic observables, that characterizes the deviation of the system from the conformal limit, where the energy density (ε) equals 3 times the pressure ($3P$). In the ideal case or in the noninteracting case, *i.e.* when the quarks and gluons are idealized to be noninteracting, massless and there is no net baryon number in the system, the trace anomaly vanishes and the conformal symmetry is approached. On the other hand, if the trace anomaly is finite, it describes the existence of interaction between partons and the generation of mass. It has been observed that the trace anomaly could approach zero for large values of the temperature in QCD due to the asymptotic freedom [75]. The study on the variation of the trace anomaly with the temperature is also very important in determining the phase transition temperature. In this work, we have explored how the trace anomaly gets altered by the rotation of the

QGP medium. The trace anomaly or interaction measure is defined as

$$\begin{aligned}
\Gamma &= \varepsilon - 3P \\
&= u_\mu T^{\mu\nu} u_\nu + \Delta_{\mu\nu} T^{\mu\nu} \\
&= \frac{1}{2\pi^2} \sum_f g_f \int dp \left(p^2 \omega_f - \frac{p^4}{\omega_f} \right) [f_0^q \chi_q(\beta\omega) + \bar{f}_0^q \chi_{\bar{q}}(\beta\omega)] \\
&\quad + \frac{1}{2\pi^2} g_g \int dp \left(p^2 \omega_g - \frac{p^4}{\omega_g} \right) f_0^g \chi_g(\beta\omega).
\end{aligned} \tag{58}$$

The thermal diffusion constant (D^T) is associated with the rate of heat transfer in a system. It appears in the diffusion equation for heat as

$$\frac{\partial T}{\partial t} = D^T \nabla^2 T, \tag{59}$$

which is carried out at constant pressure. The thermal diffusion constant in the first order relativistic viscous hydrodynamics can be defined in terms of the thermal conductivity and the specific heat at constant pressure as

$$D^T = \frac{\kappa}{C_P}. \tag{60}$$

Larger value of the thermal diffusion constant reflects the fact that the heat transfer is faster in the medium. Through κ (45) and C_P (56), it is possible to discern the influence of rotation on the thermal diffusion constant in QGP medium.

Another important observable is the isothermal compressibility (k^T), which can also be modulated by the rotation of the QGP medium. It acts as one of the thermodynamic response functions related to the equation of state, which governs the evolution of the system. It can also be useful in discerning the nature of the phase transition of the matter produced in heavy ion collisions. Depending on the center-of-mass energy, k^T may also change. Thermodynamically, the isothermal compressibility is defined as

$$k^T = -\frac{1}{V} \left(\frac{\partial V}{\partial P} \right)_T, \tag{61}$$

where V denotes the volume. Thus the isothermal compressibility measures how much the volume of the system decreases with the increase of pressure at a constant temperature. Generally, an increase in the applied pressure leads to a decrease in volume, so the negative sign appearing in eq. (61) makes the value of k^T positive. Smaller value of the isothermal compressibility indicates that the matter is stiffer. This observable can also provide the information about the deviation of a system from perfect fluid behavior. In heavy ion collisions, the isothermal compressibility can be calculated from the event-by-event fluctuation of charged particle multiplicity distributions [76]. For precise idea about the

equation of state of the system, k^T has utmost significance. For calculation, the isothermal compressibility can be transformed into a tractable form as

$$\begin{aligned} k^T &= \frac{1}{n} \left(\frac{\partial n}{\partial P} \right)_T \\ &= \frac{1}{n} \left(\frac{\partial n / \partial \mu}{\partial P / \partial \mu} \right)_T. \end{aligned} \quad (62)$$

Here, the expressions of n , $\partial n / \partial \mu$ and $\partial P / \partial \mu$ are respectively written as

$$n = \frac{1}{2\pi^2} \sum_f g_f \int d\mathbf{p} \, p^2 [f_0^q \chi_q(\beta\omega) + \bar{f}_0^q \chi_{\bar{q}}(\beta\omega)] + \frac{1}{2\pi^2} g_g \int d\mathbf{p} \, p^2 f_0^g \chi_g(\beta\omega), \quad (63)$$

$$\frac{\partial n}{\partial \mu} = \frac{\beta}{2\pi^2} \sum_f g_f \int d\mathbf{p} \, p^2 [f_0^q (1 - f_0^q) \chi_q(\beta\omega) - \bar{f}_0^q (1 - \bar{f}_0^q) \chi_{\bar{q}}(\beta\omega)], \quad (64)$$

$$\frac{\partial P}{\partial \mu} = \frac{\beta}{6\pi^2} \sum_f g_f \int d\mathbf{p} \, \frac{p^4}{\omega_f} [f_0^q (1 - f_0^q) \chi_q(\beta\omega) - \bar{f}_0^q (1 - \bar{f}_0^q) \chi_{\bar{q}}(\beta\omega)]. \quad (65)$$

The isothermal compressibility at finite rotation can be obtained by using the values of n , $\partial n / \partial \mu$ and $\partial P / \partial \mu$ in eq. (62) in the similar regime.

3 Results and discussions

In the present work, the quasiparticle masses or the thermal masses of particles within the quasiparticle model are considered. These masses are generated due to the interactions of partons with the surrounding thermal medium. At finite temperature and finite chemical potential, the quasiparticle masses (squared) of quark and gluon up to one-loop are given [77–79] by

$$m_{fT}^2 = \frac{g^2 T^2}{6} \left(1 + \frac{\mu_f^2}{\pi^2 T^2} \right), \quad (66)$$

$$m_{gT}^2 = \frac{g^2 T^2}{6} \left(N_c + \frac{N_f}{2} + \frac{3}{2\pi^2 T^2} \sum_f \mu_f^2 \right), \quad (67)$$

respectively. Here, g is the one-loop running coupling with the following [80] form,

$$g^2 = 4\pi\alpha_s = \frac{48\pi^2}{(11N_c - 2N_f) \ln \left(\Lambda^2 / \Lambda_{\overline{\text{MS}}}^2 \right)}, \quad (68)$$

where $\Lambda_{\overline{\text{MS}}} = 0.176 \text{ GeV}$, $\Lambda = 2\pi\sqrt{T^2 + \mu_f^2/\pi^2}$ for electrically charged particles (quarks and antiquarks) and $\Lambda = 2\pi T$ for gluons. In this work, the value of the chemical potential is set at 0.06 GeV.

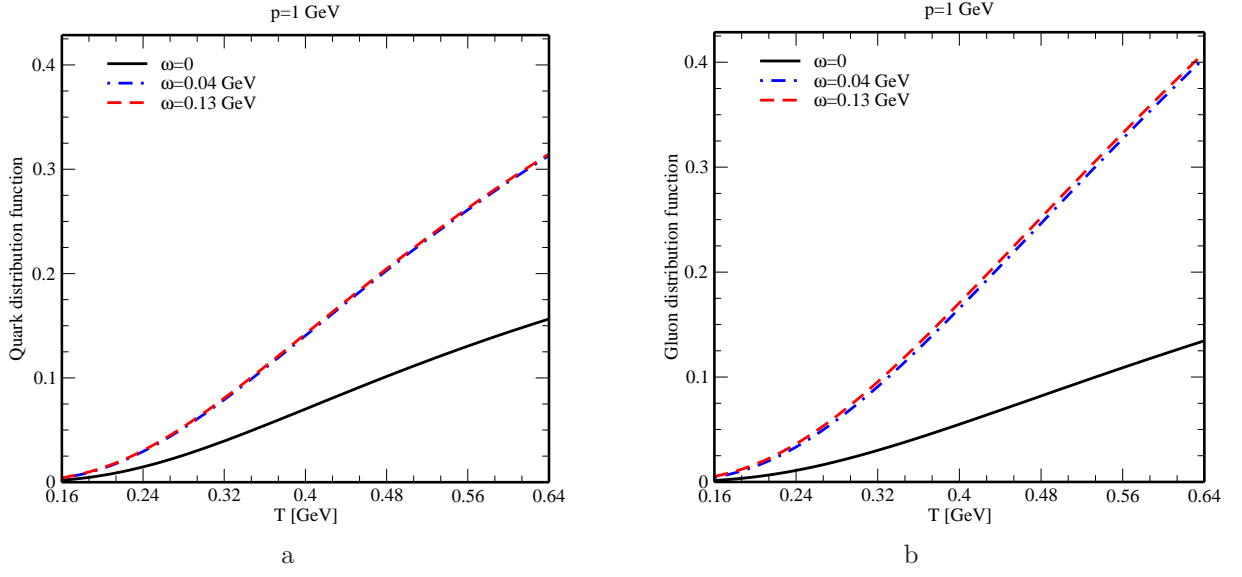


Figure 1: Temperature dependence of (a) quark and (b) gluon distribution functions for different values of angular velocity.

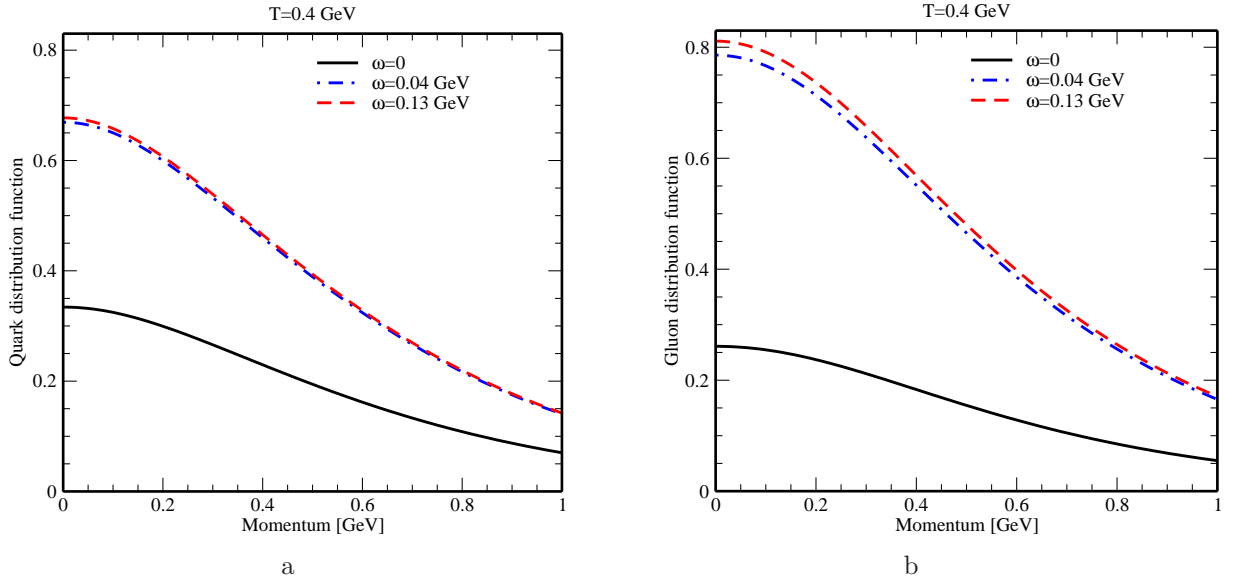


Figure 2: Momentum dependence of (a) quark and (b) gluon distribution functions for different values of angular velocity.

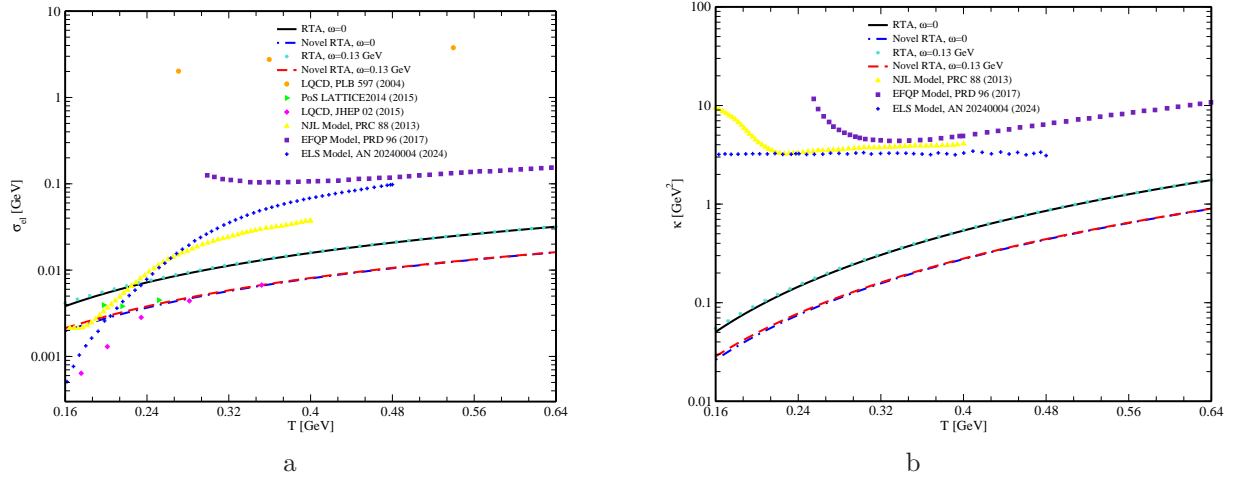


Figure 3: Variation of (a) the electrical conductivity and (b) the thermal conductivity with temperature for different values of angular velocity.

To understand the effect of rotational QGP medium on the transport coefficients and observables, let us first observe how the particle distribution functions get altered in the similar environment. Figure 1 shows the temperature dependence of the u quark and gluon distribution functions at a fixed momentum for different values of the angular velocity, whereas figure 2 displays the momentum dependence of these distribution functions at a fixed temperature for different angular velocities. From the observation on the distribution functions, it is inferred that the parton number densities can increase with the increase of angular velocity. The effect of rotation on parton distribution functions is more evident at high temperatures and low momenta. It can be further noticed from figures 1 and 2 that, as compared to the quark distribution function, the gluon distribution function is more influenced by the rotation of the QGP medium. This can be perceived from the fact that the number of gluons in adjoint representation is larger than the number of quarks in fundamental representation at high temperatures, so the overall response of gluons to rotation exceeds that of quarks. These observations on the parton distribution functions would help greatly in exploring the effect of rotation on various transport coefficients and observables in kinetic theory approach.

Figure 3 depicts the variation of electrical (σ_{el}) and thermal (κ) conductivities of the QGP medium with temperature for different values of angular velocity in the relaxation time approximation as well as in the novel relaxation time approximation. Observation shows that the emergence of angular velocity gives an increasing effect to both σ_{el} and κ , and their deviations from $\omega = 0$ case are less prominent at high temperatures. In the novel relaxation time approximation, a decrease in σ_{el} and κ is observed as compared to the frequently used relaxation time approximation. Difference between the results in these two approximations is mainly attributed to the different relaxation times and collision

integrals in both cases. From figures 3a and 3b, it is seen that the distinction between the RTA and the novel RTA is more conspicuous at higher temperatures both for the nonrotating and rotating QGP mediums. Thus the rotation facilitates the transport of charge and heat in the medium.

We have also compared our results with the results obtained from other models, such as the lattice QCD [81–83], the Nambu-Jona-Lasinio (NJL) model [84], the effective fugacity quasiparticle (EFQP) model [85] and the extended linear sigma (ELS) model [86]. We note that the aforesaid models including the lattice simulation with the rotation are at an early stage of development, and the results on electrical and thermal conductivities at finite rotation are not yet available in these models, so we have used the results in the absence of rotation from these models. The electrical conductivity in the hot phase of the QCD plasma is extracted from a quenched lattice measurement of the Euclidean time vector correlator for $1.5 \leq T/T_c \leq 3$ in ref. [81]. This study estimates the value of the electrical conductivity that lies above our results at zero angular velocity as well as at finite angular velocity. In ref. [82], the electrical conductivity has been calculated using the vector correlation function within the quenched lattice QCD and this result is found to be in close proximity to our results throughout the considered temperature range. Lattice result in ref. [83] lies slightly below our result calculated using RTA method, whereas it is closer to our result determined using the novel RTA method. Upon comparing our results with the NJL model [84], EFQP model [85] and ELS model [86] calculations, it is found that the results of the aforesaid models lie above our results on electrical conductivity in the absence as well as in the presence of finite angular velocity. However, as compared to the EFQP model, the NJL model and the ELS model estimations on electrical conductivity are in close agreement with our results at low temperatures. We note that the lattice QCD calculations on the thermal conductivity are not available in literature, so we have only compared our results on the thermal conductivity with that in the NJL model [84], EFQP model [85] and ELS model [86]. We have found that the results from these models lie above our result over the entire range of temperature for both nonrotating and rotating medium cases. However at high temperatures, our result on the thermal conductivity is closer to the estimations of these models.

In figure 4, the effects of rotation on the Knudsen number (Ω) and the elliptic flow (v_2) have been displayed. Observation shows a decrease in the Knudsen number (figure 4a) and an increase in the elliptic flow (figure 4b) when rotation is introduced in the medium. This behavior of the Knudsen number at finite angular velocity is corroborated by the observations on the thermal conductivity and the specific heat at constant volume in the similar regime. The increase of v_2 at finite rotation also agrees with the observation in ref. [6]. Thus the medium approaches towards the equilibrium with the increase of rotation. Further, the novel relaxation time approximation estimates smaller value of Ω

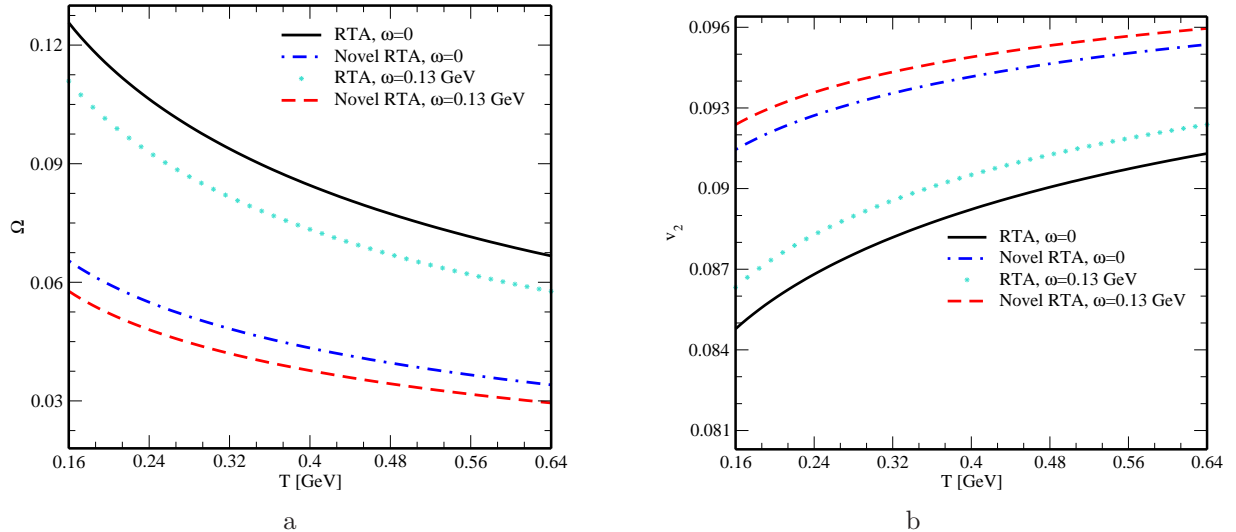


Figure 4: Variation of (a) the Knudsen number and (b) the elliptic flow with temperature for different values of angular velocity.

and larger value of v_2 as compared to their corresponding values in the relaxation time approximation. This indicates an enhancement of the interactions among the produced particles in heavy ion collisions and faster thermalization of the medium.

Figure 5 shows the effects of rotation on the specific heat at constant pressure (C_P) and the specific heat at constant volume (C_V) over a given range of the temperature. It is observed that the emergence of rotation enhances both C_P and C_V , with the magnitude of the former being larger than that of the latter for all temperatures. Thus, for a rotating medium, the changes in enthalpy and energy density with temperature are larger as compared to the nonrotating case. The relative behavior between C_P and C_V can be discerned through their ratio γ or the adiabatic index. Figure 6 displays how the adiabatic index varies with temperature and with angular velocity. It is observed that the adiabatic index becomes larger as the medium gets hotter, whereas, if the rotation is introduced into the medium, γ gets decreased as compared to the $\omega = 0$ case (figure 6a). On the other hand, within the rotating medium, γ is found to increase with the increase of angular velocity. Further, the trend of variation of γ with the angular velocity is not same for all temperatures, rather the increase of γ with angular velocity becomes faster for lower temperatures (figure 6b). In low angular velocity regime, the variation of γ is meagre, however, a noticeable increasing behavior of γ is observed in high angular velocity regime. This indicates that the change in enthalpy is larger than the change in energy density for an increase of one unit in temperature and this difference gets enhanced as the rotation of the QGP medium becomes more rapid.

In figure 7, the variation of the trace anomaly in units of its value in the absence of

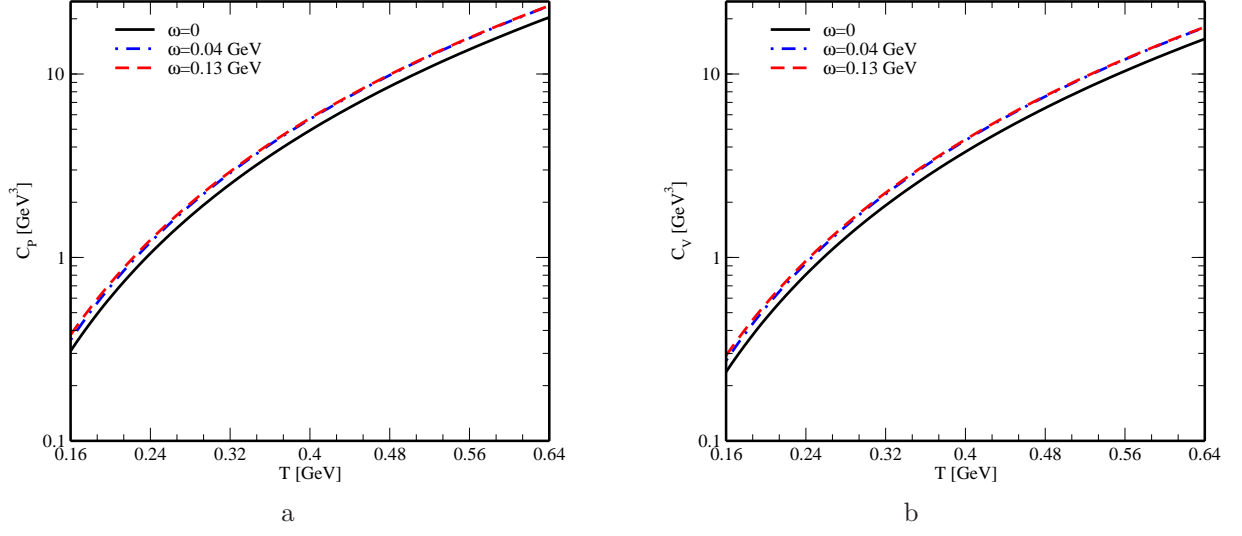


Figure 5: Variation of (a) the specific heat at constant pressure and (b) the specific heat at constant volume with temperature for different values of angular velocity.

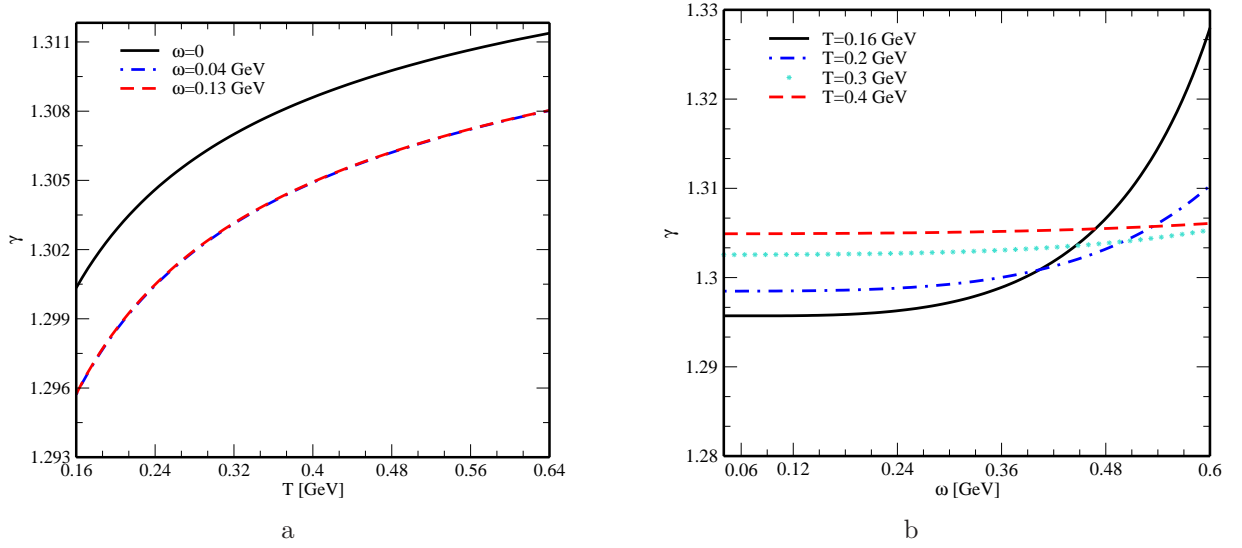


Figure 6: Variation of the ratio γ (C_P/C_V) (a) with temperature for different values of angular velocity and (b) with angular velocity for different values of temperature.

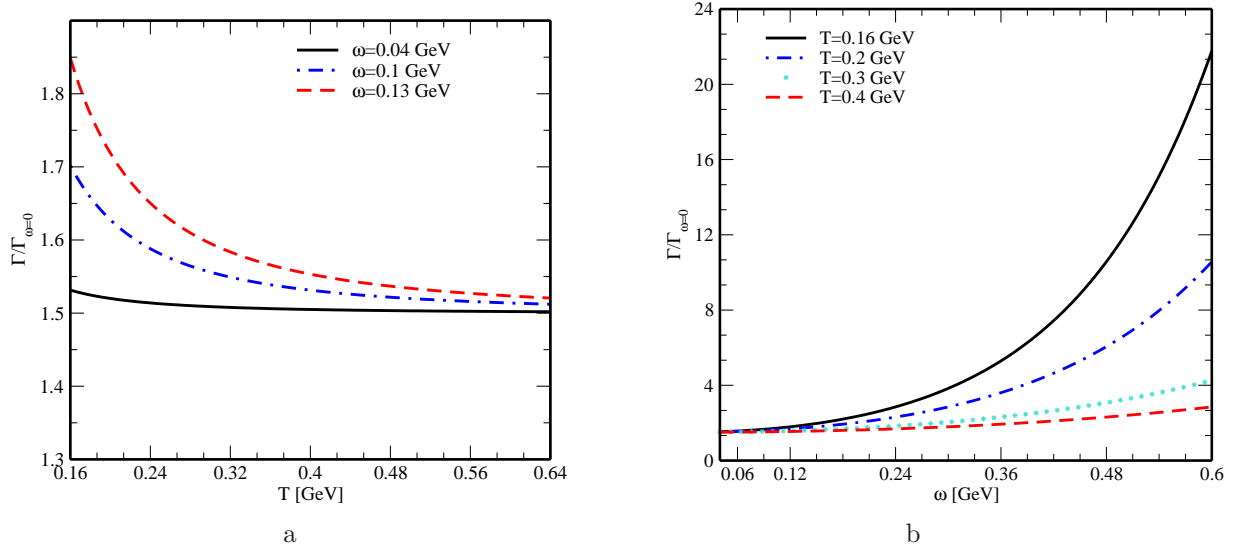


Figure 7: Variation of the trace anomaly scaled with its value in the absence of rotation (a) as a function of temperature for different values of angular velocity and (b) as a function of angular velocity for different values of temperature.

rotation with temperature and with angular velocity has been depicted. It is observed that, with the increase of temperature, the deviation of the trace anomaly at finite angular velocity from that at zero angular velocity decreases (figure 7a). Thus, at high temperatures, rotation of the medium has a meagre impact on the trace anomaly. Our observation has further found an increasing trend of the trace anomaly as the angular velocity increases and the slope decreases if the medium becomes hotter (figure 7b). The effect of angular velocity on the trace anomaly seems to be more pronounced at lower temperatures. Thus the rotation makes the constituents of the medium more interactive and as a result, it takes the medium a bit away from the conformal symmetry.

Figure 8 displays how the thermal diffusion constant (D^T) and the isothermal compressibility (κ^T) get modulated by the rotation with varying temperature. It is observed that the rotation of the medium reduces the thermal diffusion constant over the entire range of temperature (figure 8a). This reduction in D^T is mainly attributed to the variations of κ and C_P in the similar regime. With the angular velocity, the increase in the specific heat at constant pressure dominates over the increase in the thermal conductivity, therefore, a decrease in the thermal diffusion constant at finite angular velocity is observed. Smaller value of the thermal diffusion constant indicates slower heat transfer in a rotating medium as compared to that in a nonrotating medium. With the increase of the temperature, the isothermal compressibility is found to decrease (figure 8b). Further, the introduction of angular velocity also reduces the isothermal compressibility and the matter may show nearly perfect fluid behavior. This suggests that, with the increasing

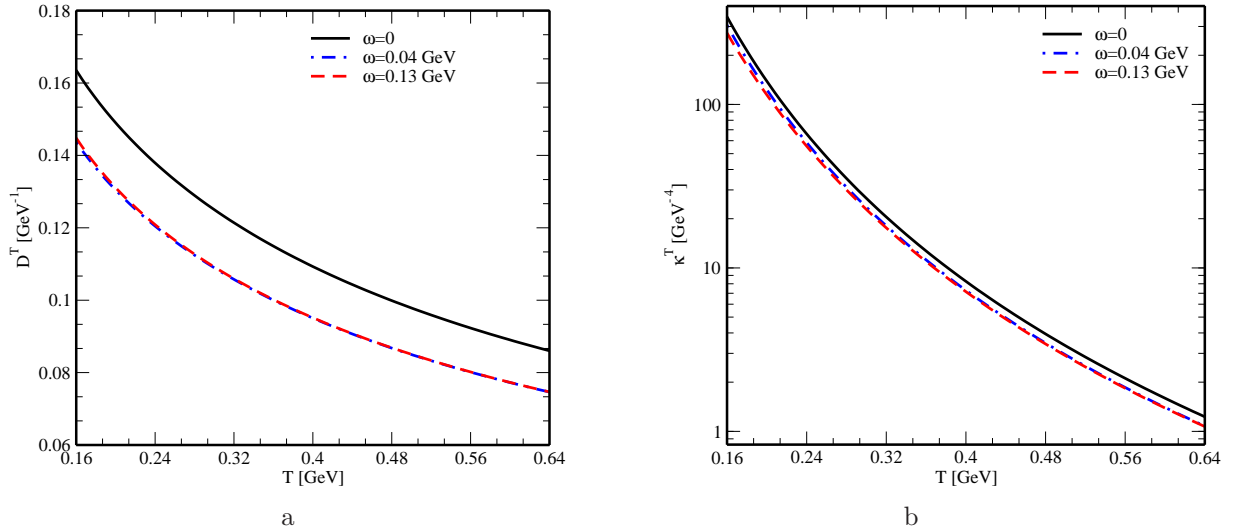


Figure 8: Variation of (a) the thermal diffusion constant and (b) the isothermal compressibility with temperature for different values of angular velocity.

angular velocity, it is difficult to compress the system. Thus, it is inferred that the matter becomes stiffer as the rotation becomes more rapid.

4 Conclusions

In this work, we explored the transport coefficients and observables of a rotating QGP medium. We calculated the electrical and thermal conductivities using the relativistic Boltzmann transport equation in the novel relaxation time approximation within the kinetic theory approach. We also compared our results with the frequently used relaxation time approximation. We observed that the introduction of rotation enhances the conduction of charge and heat in the medium. In addition, the novel relaxation time approximation estimates smaller values of the electrical and thermal conductivities as compared to their corresponding values in the relaxation time approximation. We further explored the effects of rotation on various observables, such as the Knudsen number, the elliptic flow, the specific heat at constant pressure, the specific heat at constant volume, the trace anomaly, the thermal diffusion constant and the isothermal compressibility. From the behavior of these observables, we found that the rotation leaves a significant influence on the equilibrium property of the medium, the interactions among particles produced in heavy ion collisions, the adiabatic index, the conformal symmetry, the rate of heat transfer in the medium and the stiffness of the medium.

Acknowledgments

One of the present authors (S. R.) acknowledges financial support from ANID Fondecyt postdoctoral grant 3240349 and S. D. acknowledges the SERB Power Fellowship, SPF/2022/000014 for the support on this work.

References

- [1] W. T. Deng and X. G. Huang, *Vorticity in heavy-ion collisions*, Phys. Rev. C **93**, 064907 (2016).
- [2] Y. Jiang, Z. W. Lin and J. Liao, *Rotating quark-gluon plasma in relativistic heavy-ion collisions*, Phys. Rev. C **94**, 044910 (2016).
- [3] X. Wang, M. Wei, Z. Li and M. Huang, *Quark matter under rotation in the NJL model with vector interaction*, Phys. Rev. D **99**, 016018 (2019).
- [4] M. Wei, C. A. Islam and M. Huang, *Production rate and ellipticity of lepton pairs from a rotating hot and dense QCD medium*, Phys. Rev. D **105**, 054014 (2022).
- [5] Z. T. Liang and X. N. Wang, *Spin alignment of vector mesons in non-central $A + A$ collisions*, Phys. Lett. B **629**, 20 (2005).
- [6] F. Becattini, F. Piccinini and J. Rizzo, *Angular momentum conservation in heavy ion collisions at very high energy*, Phys. Rev. C **77**, 024906 (2008).
- [7] E. Berti, F. White, A. Maniopoulou and M. Bruni, *Rotating neutron stars: an invariant comparison of approximate and numerical space-time models*, Mon. Not. R. Astron. Soc. **358**, 923 (2005).
- [8] A. L. Fetter, *Rotating trapped Bose-Einstein condensates*, Rev. Mod. Phys. **81**, 647 (2009).
- [9] D. E. Kharzeev and D. T. Son, *Testing the Chiral Magnetic and Chiral Vortical Effects in Heavy Ion Collisions*, Phys. Rev. Lett. **106**, 062301 (2011).
- [10] D. T. Son and P. Surowka, *Hydrodynamics with Triangle Anomalies*, Phys. Rev. Lett. **103**, 191601 (2009).
- [11] Y. Jiang, X. G. Huang and J. Liao, *Chiral vortical wave and induced flavor charge transport in a rotating quark-gluon plasma*, Phys. Rev. D **92**, 071501 (2015).
- [12] K. Fukushima, D. E. Kharzeev and H. J. Warringa, *Chiral magnetic effect*, Phys. Rev. D **78**, 074033 (2008).

- [13] D. E. Kharzeev, L. D. McLerran and H. J. Warringa, *The effects of topological charge change in heavy ion collisions: “Event by event P and CP violation”*, Nucl. Phys. A **803**, 227 (2008).
- [14] D. E. Kharzeev and H. U. Yee, *Chiral magnetic wave*, Phys. Rev. D **83**, 085007 (2011).
- [15] Y. Burnier, D. E. Kharzeev, J. Liao and H. U. Yee, *Chiral Magnetic Wave at Finite Baryon Density and the Electric Quadrupole Moment of the Quark-Gluon Plasma*, Phys. Rev. Lett. **107**, 052303 (2011).
- [16] A. Ipp, A. Di Piazza, J. Evers and C. H. Keitel, *Photon polarization as a probe for quark-gluon plasma dynamics*, Phys. Lett. B **666**, 315 (2008).
- [17] B. Betz, M. Gyulassy and G. Torrieri, *Polarization probes of vorticity in heavy ion collisions*, Phys. Rev. C **76**, 044901 (2007).
- [18] F. Becattini and F. Piccinini, *The ideal relativistic spinning gas: Polarization and spectra*, Ann. Phys. (Amsterdam) **323**, 2452 (2008).
- [19] F. Becattini, V. Chandra, L. D. Zanna and E. Grossi, *Relativistic distribution function for particles with spin at local thermodynamical equilibrium*, Ann. Phys. **338**, 32 (2013).
- [20] W. Florkowski, A. Kumar and R. Ryblewski, *Relativistic hydrodynamics for spin-polarized fluids*, Prog. Part. Nucl. Phys. **108**, 103709 (2019).
- [21] S. Bhadury, W. Florkowski, A. Jaiswal, A. Kumar and R. Ryblewski, *Relativistic Spin Magnetohydrodynamics*, Phys. Rev. Lett. **129**, 192301 (2022).
- [22] V. E. Ambruş, R. Ryblewski and R. Singh, *Spin waves in spin hydrodynamics*, Phys. Rev. D **106**, 014018 (2022).
- [23] F. Becattini and M. A. Lisa, *Polarization and Vorticity in the Quark-Gluon Plasma*, Ann. Rev. Nucl. Part. Sci. **70**, 395 (2020).
- [24] A. Vilenkin, *Quantum field theory at finite temperature in a rotating system*, Phys. Rev. D **21**, 2260 (1980).
- [25] M. N. Chernodub and S. Gongyo, *Interacting fermions in rotation: chiral symmetry restoration, moment of inertia and thermodynamics*, J. High Energy Phys. **1701**, 136 (2017).
- [26] S. Ebihara, K. Fukushima and K. Mameda, *Boundary effects and gapped dispersion in rotating fermionic matter*, Phys. Lett. B **764**, 94 (2017).

- [27] Y. Fujimoto, K. Fukushima and Y. Hidaka, *Deconfining phase boundary of rapidly rotating hot and dense matter and analysis of moment of inertia*, Phys. Lett. B **816**, 136184 (2021).
- [28] X. Chen, L. Zhang, D. Li, D. Hou and M. Huang, *Gluodynamics and deconfinement phase transition under rotation from holography*, J. High Energy Phys. **2107**, 132 (2021).
- [29] V. V. Braguta, A. Y. Kotov, D. D. Kuznedeleev and A. A. Roenko, *Study of the Confinement/Deconfinement Phase Transition in Rotating Lattice $SU(3)$ Gluodynamics*, JETP Lett. **112**, 9 (2020).
- [30] V. V. Braguta, A. Y. Kotov, D. D. Kuznedeleev and A. A. Roenko, *Influence of relativistic rotation on the confinement-deconfinement transition in gluodynamics*, Phys. Rev. D **103**, 094515 (2021).
- [31] Y. Jiang and J. Liao, *Pairing Phase Transitions of Matter under Rotation*, Phys. Rev. Lett. **117**, 192302 (2016).
- [32] B. R. Iyer, *Dirac field theory in rotating coordinates*, Phys. Rev. D **26**, 1900 (1982).
- [33] F. Becattini and L. Tinti, *Thermodynamical inequivalence of quantum stress-energy and spin tensors*, Phys. Rev. D **84**, 025013 (2011).
- [34] V. E. Ambruş and E. Winstanley, *Rotating quantum states*, Phys. Lett. B **734**, 296 (2014).
- [35] V. E. Ambruş and E. Winstanley, *Rotating fermions inside a cylindrical boundary*, Phys. Rev. D **93**, 104014 (2016).
- [36] H. -L. Chen, K. Fukushima, X. -G. Huang and K. Mameda, *Analogy between rotation and density for Dirac fermions in a magnetic field*, Phys. Rev. D **93**, 104052 (2016).
- [37] B. McInnes, *Angular momentum in QGP holography*, Nucl. Phys. B **887**, 246 (2014).
- [38] B. McInnes, *A rotation/magnetism analogy for the quark-gluon plasma*, Nucl. Phys. B **911**, 173 (2016).
- [39] B. Singh, J. R. Bhatt and H. Mishra, *Probing vorticity in heavy ion collision with dilepton production*, Phys. Rev. D **100**, 014016 (2019).
- [40] S. Rath and B. K. Patra, *Revisit to electrical and thermal conductivities, Lorenz and Knudsen numbers in thermal QCD in a strong magnetic field*, Phys. Rev. D **100**, 016009 (2019).
- [41] S. Rath and B. K. Patra, *One-loop QCD thermodynamics in a strong homogeneous and static magnetic field*, J. High Energy Phys. **1712**, 098 (2017).

- [42] A. Bandyopadhyay, B. Karmakar, N. Haque and M. G. Mustafa, *Pressure of a weakly magnetized hot and dense deconfined QCD matter in one-loop hard-thermal-loop perturbation theory*, Phys. Rev. D **100**, 034031 (2019).
- [43] S. Rath and B. K. Patra, *Thermomagnetic properties and Bjorken expansion of hot QCD matter in a strong magnetic field*, Eur. Phys. J. A **55**, 220 (2019).
- [44] B. Karmakar, R. Ghosh, A. Bandyopadhyay, N. Haque and M. G. Mustafa, *Anisotropic pressure of deconfined QCD matter in presence of strong magnetic field within one-loop approximation*, Phys. Rev. D **99**, 094002 (2019).
- [45] B. Feng, *Electric conductivity and Hall conductivity of the QGP in a magnetic field*, Phys. Rev. D **96**, 036009 (2017).
- [46] S. Rath and S. Dash, *Effects of weak magnetic field and finite chemical potential on the transport of charge and heat in hot QCD matter*, Eur. Phys. J. A **59**, 25 (2023).
- [47] K. Hattori and D. Satow, *Electrical conductivity of quark-gluon plasma in strong magnetic fields*, Phys. Rev. D **94**, 114032 (2016).
- [48] K. Fukushima and Y. Hidaka, *Electric Conductivity of Hot and Dense Quark Matter in a Magnetic Field with Landau Level Resummation via Kinetic Equations*, Phys. Rev. Lett. **120**, 162301 (2018).
- [49] S. Rath and B. K. Patra, *Effect of magnetic field on the charge and thermal transport properties of hot and dense QCD matter*, Eur. Phys. J. C **80**, 747 (2020).
- [50] M. Kurian, S. Mitra, S. Ghosh and V. Chandra, *Transport coefficients of hot magnetized QCD matter beyond the lowest Landau level approximation*, Eur. Phys. J. C **79**, 134 (2019).
- [51] G. S. Denicol *et al.*, *Nonresistive dissipative magnetohydrodynamics from the Boltzmann equation in the 14-moment approximation*, Phys. Rev. D **98**, 076009 (2018).
- [52] Seung-i. Nam and Chung-W. Kao, *Shear viscosity of quark matter at finite temperature under an external magnetic field*, Phys. Rev. D **87**, 114003 (2013).
- [53] S. Rath and S. Dash, *Momentum transport properties of a hot and dense QCD matter in a weak magnetic field*, Eur. Phys. J. C **82**, 797 (2022).
- [54] S. Rath and B. K. Patra, *Momentum and its affiliated transport coefficients for hot QCD matter in a strong magnetic field*, Phys. Rev. D **102**, 036011 (2020).
- [55] S. Rath and B. K. Patra, *Viscous properties of hot and dense QCD matter in the presence of a magnetic field*, Eur. Phys. J. C **81**, 139 (2021).

- [56] K. Hattori, X.-G. Huang, D. H. Rischke and D. Satow, *Bulk viscosity of quark-gluon plasma in strong magnetic fields*, Phys. Rev. D **96**, 094009 (2017).
- [57] S. Li and Ho-U. Yee, *Shear viscosity of the quark-gluon plasma in a weak magnetic field in perturbative QCD: Leading log*, Phys. Rev. D **97**, 056024 (2018).
- [58] H. van Hees, C. Gale and R. Rapp, *Thermal photons and collective flow at energies available at the BNL Relativistic Heavy-Ion Collider*, Phys. Rev. C **84**, 054906 (2011).
- [59] C. Shen, U. W. Heinz, J.-F. Paquet and C. Gale, *Thermal photons as a quark-gluon plasma thermometer reexamined*, Phys. Rev. C **89**, 044910 (2014).
- [60] K. Tuchin, *Magnetic contribution to dilepton production in heavy-ion collisions*, Phys. Rev. C **88**, 024910 (2013).
- [61] K. A. Mamo, *Enhanced thermal photon and dilepton production in strongly coupled $N = 4$ SYM plasma in strong magnetic field*, J. High Energy Phys. **1308**, 083 (2013).
- [62] K. Fukushima, K. Hattori, H.-U. Yee and Y. Yin, *Heavy quark diffusion in strong magnetic fields at weak coupling and implications for elliptic flow*, Phys. Rev. D **93**, 074028 (2016).
- [63] C. Cercignani and G. M. Kremer. “The Relativistic Boltzmann Equation: Theory and Applications”. Birkhäuser Basel, 2002.
- [64] G. S. Rocha, G. S. Denicol and J. Noronha, *Novel Relaxation Time Approximation to the Relativistic Boltzmann Equation*, Phys. Rev. Lett. **127**, 042301 (2021).
- [65] F. Becattini and L. Tinti, *The ideal relativistic rotating gas as a perfect fluid with spin*, Ann. Phys. **325**, 1566 (2010).
- [66] F. Becattini and L. Ferroni, *The microcanonical ensemble of the ideal relativistic quantum gas with angular momentum conservation*, Eur. Phys. J. C **52**, 597 (2007).
- [67] A. Hosoya and K. Kajantie, *Transport coefficients of QCD matter*, Nucl. Phys. B **250**, 666 (1985).
- [68] K. Dusling, G. D. Moore and D. Teaney, *Radiative energy loss and v_2 spectra for viscous hydrodynamics*, Phys. Rev. C **81**, 034907 (2010).
- [69] E. Calzetta and B. L. Hu, *Nonequilibrium quantum fields: Closed-time-path effective action, Wigner function, and Boltzmann equation*, Phys. Rev. D **37**, 2878 (1988).
- [70] R. S. Bhalerao, J.-P. Blaizot, N. Borghini and J.-Y. Ollitrault, *Elliptic flow and incomplete equilibration at RHIC*, Phys. Lett. B **627**, 49 (2005).

- [71] H.-J. Drescher, A. Dumitru, C. Gombeaud and J.-Y. Ollitrault, *Centrality dependence of elliptic flow, the hydrodynamic limit, and the viscosity of hot QCD*, Phys. Rev. C **76**, 024905 (2007).
- [72] C. Gombeaud and J.-Y. Ollitrault, *Covariant transport theory approach to elliptic flow in relativistic heavy ion collision*, Phys. Rev. C **77**, 054904 (2008).
- [73] S. Rath and S. Dash, *Impact of nonextensivity on the transport coefficients of a magnetized hot and dense QCD matter*, Eur. Phys. J. C **83**, 867 (2023).
- [74] R. K. Mohapatra, P. S. Saumia and A. M. Srivastava, *Enhancement of flow anisotropies due to magnetic field in relativistic heavy-ion collisions*, Mod. Phys. Lett. A **26**, 2477 (2011).
- [75] J. O. Andersen, N. Haque, M. G. Mustafa and M. Strickland, *Three-loop hard-thermal-loop perturbation theory thermodynamics at finite temperature and finite baryonic and isospin chemical potential*, Phys. Rev. D **93**, 054045 (2016).
- [76] S. Mrówczyński, *Hadronic matter compressibility from event-by-event analysis of heavy-ion collisions*, Phys. Lett. B **430**, 9 (1998).
- [77] E. Braaten and R. D. Pisarski, *Simple effective Lagrangian for hard thermal loops*, Phys. Rev. D **45**, R1827 (1992).
- [78] A. Peshier, B. Kämpfer and G. Soff, *From QCD lattice calculations to the equation of state of quark matter*, Phys. Rev. D **66**, 094003 (2002).
- [79] J.-P. Blaizot, A. Ipp, A. Rebhan and U. Reinosa, *Asymptotic thermal quark masses and the entropy of QCD in the large - N_f limit*, Phys. Rev. D **72**, 125005 (2005).
- [80] J. I. Kapusta and C. Gale. Finite Temperature Field Theory Principles and Applications (Cambridge University Press, Cambridge, 2006).
- [81] S. Gupta, *The electrical conductivity and soft photon emissivity of the QCD plasma*, Phys. Lett. B **597**, 57 (2004).
- [82] H.-T. Ding, O. Kaczmarek and F. Meyer, *Vector spectral functions and transport properties in quenched QCD*, PoS LATTICE2014, 216 (2015).
- [83] G. Aarts, C. Allton, A. Amato, P. Giudice, S. Hands and J.-I. Skullerud, *Electrical conductivity and charge diffusion in thermal QCD from the lattice*, J. High Energy Phys. **02**, 186 (2015).
- [84] R. Marty, E. Bratkovskaya, W. Cassing, J. Aichelin and H. Berrehrach, *Transport coefficients from the Nambu-Jona-Lasinio model for $SU(3)_f$* , Phys. Rev. C **88**, 045204 (2013).

- [85] S. Mitra and V. Chandra, *Transport coefficients of a hot QCD medium and their relative significance in heavy-ion collisions*, Phys. Rev. D **96**, 094003 (2017).
- [86] A. N. Tawfik and A. Elshehri, *Extended linear-sigma model: transport properties of QCD matter at finite temperature*, Astron. Nachr. **20240004** (2024).